AGU PUBLICATIONS

Geophysical Research Letters

RESEARCH LETTER
10.1002/2014GL059480

**Key Points:**
- Representative data set of acetone in the UT/LMS on a global scale from CARIBIC
- HOx production due to acetone degradation and from O3 photolysis are contrasted
- Year-around acetone is a significant source of HOx in the upper troposphere

**Correspondence to:**
M. Neumaier,
marco.neumaier@kit.edu

**Citation:**
Neumaier, M., R. Ruhnke, O. Kirner, H. Ziereis, G. Stratmann, C. A. M. Brenninkmeijer, and A. Zahn (2014), Impact of acetone (photo)oxidation on $HO_x$ production in the UT/LMS based on CARIBIC passenger aircraft observations and EMAC simulations, *Geophys. Res. Lett.*, *41*, 3289–3297, doi:10.1002/2014GL059480.

Received 3 FEB 2014
Accepted 28 MAR 2014
Accepted article online 1 APR 2014
Published online 1 MAY 2014

# Impact of acetone (photo)oxidation on $HO_x$ production in the UT/LMS based on CARIBIC passenger aircraft observations and EMAC simulations

**M. Neumaier[1], R. Ruhnke[1], O. Kirner[2], H. Ziereis[3], G. Stratmann[3], C. A. M. Brenninkmeijer[4], and A. Zahn[1]**

[1]Karlsruhe Institute of Technology (KIT), Institute of Meteorology and Climate Research (IMK-ASF), Karlsruhe, Germany, [2]Karlsruhe Institute of Technology (KIT), Steinbuch Centre for Computing (SCC), Karlsruhe, Germany, [3]Deutsches Zentrum für Luft- und Raumfahrt (DLR), Institute of Atmospheric Physics, Wessling, Germany, [4]Max Planck Institute for Chemistry (MPIC), Air Chemistry Division, Mainz, Germany

**Abstract** Until a decade ago, acetone was assumed to be a dominant $HO_x$ source in the dry extra-tropical upper troposphere (ex-UT). New photodissociation quantum yields of acetone and the lack of representative data from the ex-UT challenged that assumption. Regular mass spectrometric observations onboard the Civil Aircraft for the Regular Investigation of the atmosphere Based on an Instrument Container (CARIBIC) passenger aircraft deliver the first representative distribution of acetone in the UT/LMS (UT/lowermost stratosphere). Based on diverse CARIBIC trace gas data and non-observed parameters taken from the model ECHAM5/MESSy for Atmospheric Chemistry, we quantify the $HO_x$ source in the UT/LMS from (photo)oxidation of acetone. The findings are contrasted to $HO_x$ production from ozone photolysis, overall the dominant tropospheric $HO_x$ source. It is shown that $HO_x$ production from acetone (photo)oxidation reaches up to 95% of the $HO_x$ source from ozone photolysis in autumn in the UT and on average ~61% in summer. That is, acetone is a significant source of $HO_x$ in the UT/LMS.

## 1. Introduction

$HO_x$ radicals ($HO_x = OH + HO_2$) govern the chemical lifetime of basically all organic species and many other crucial trace gases such as $CH_4$ and CO and thus largely control the oxidative capacity of the troposphere [e.g., *Prinn*, 2003]. The main primary source of OH near ground and in the mid-troposphere is reaction of $O^1D$ (formed *via* photolysis of ozone ($O_3$)) with water ($H_2O$), in the following denoted as $O_3$-$HO_x$ source [*Folkins and Chatfield*, 2000; *Jaeglé et al.*, 2000; *Monks*, 2005]. This source becomes less dominant in the UT/lowermost stratosphere (LMS) due to the rapid decrease of $H_2O$ with altitude, whereas other $HO_x$ precursors like formaldehyde ($CH_2O$), methyl hydroperoxide ($CH_3OOH$), or acetone ($CH_3C(O)CH_3$) are gaining importance [*Folkins and Chatfield*, 2000].

Acetone photolysis was first suggested in a pioneering study by *Singh et al.* [1995] to be an important $HO_x$ source in the mid-latitude UT. This hypothesis was confirmed by subsequent studies [*Arnold et al.*, 1997; *Jaeglé et al.*, 1997; *Wennberg et al.*, 1998; *Müller and Brasseur*, 1999; *Folkins and Chatfield*, 2000; *Jaeglé et al.*, 2001]. However, the picture began to alter with the laboratory measurements of new temperature-dependent photolysis quantum yields (QYs) of acetone by *Blitz et al.* [2004]. As shown by *Arnold et al.* [2004, 2005], the reduced QYs result in acetone photolysis rates which are a factor of 3–10 smaller in the upper troposphere, compared to previously recommended photolysis rates based on QYs from *Gierczak et al.* [1998].

The reduced QYs obtained by *Blitz et al.* [2004] at long wavelengths and low temperatures, presently also recommended by expert panels [*Atkinson et al.*, 2006; *Sander et al.*, 2011], have recently been substantiated by *Nádasdi et al.* [2007] and *Khamaganov and Crowley* [2013], confirming that the importance of acetone as $HO_x$ precursor was indeed overestimated in the past.

A further crucial shortcoming in quantifying the role of acetone was the lack of representative data from the UT/LMS. This deficit can now largely be ameliorated by the CARIBIC (Civil Aircraft for the Regular Investigation of the atmosphere Based on an Instrument Container) project which delivers the largest in situ data set of acetone from the UT/LMS on a nearly world-wide scale [*Sprung and Zahn*, 2010].

The objective of this paper is to quantify the $HO_x$ source from (photo)oxidation (i.e., photolysis and reaction with OH) of acetone in the UT/LMS and compare it to the $O_3$-$HO_x$ source. As a basis, we used representative tropopause-referenced distributions of acetone, $O_3$, water vapor, and NO (which controls the yield of $HO_x$ from acetone degradation) as measured onboard CARIBIC. Parameters not accessible via the CARIBIC project, i.e., photolysis rates, the OH and $HO_2$ field, and the temperature field, were taken from the global chemistry model EMAC (ECHAM5/MESSy for Atmospheric Chemistry) [*Jöckel et al*., 2006]. In a sensitivity study, we investigated the uncertainty of our findings, and it will be demonstrated that besides the photolysis rates of acetone and ozone, the acetone distribution is the most sensitive input parameter.

## 2. Experimental

In CARIBIC, a modified airfreight container equipped with 15 instruments for measurement of altogether ~100 trace gases and aerosol parameters is deployed onboard a passenger aircraft (Lufthansa, Airbus 340-600) during a sequence of two to six flights per month [*Brenninkmeijer et al*., 2007]. The data analyzed here were collected at 9–12 km altitude (300–200 hPa), at 35°N–60°N and 124°W–142°E from 2005 to 2014. Among the most frequent flight destinations were Guangzhou (China), Caracas (Venezuela), Manila (Philippines), Chennai (India), and Vancouver (Canada) (overview available at http://www.caribic.de/2005/Flight_Scheduling.html). The systematic and long-term nature of the CARIBIC data enables, e.g., the inference of seasonal variations. Moreover, the data cover a large part of the globe and altogether provide fairly representative distributions of trace species in the UT/LMS. For acetone, data from 185 flights were considered here, for $O_3$ and $H_2O$ ~318 and for NO 177 flights. The smaller number for acetone and NO is because of occasional technical problems. Onboard CARIBIC, acetone is measured by a proton-transfer-reaction mass spectrometer which is a considerably modified version of a commercial instrument from Ionicon (Innsbruck, Austria); see *Brenninkmeijer et al*. [2007] and *Sprung and Zahn* [2010]. Protonated acetone is detected at 59 amu. Isobaric propanal has a much smaller lifetime compared to acetone (~9 h vs. ~5 weeks), has a weaker source, and can thus be neglected in the UT/LMS [*Warneke et al*., 2003]. The computed proton affinity of likewise isobaric glyoxal ($C_2H_2O_2$) is too low to be effectively ionized by proton transfer from $H_3O^+$ [*Wróblewski et al*., 2007].

Ozone was measured by two instruments, an accurate UV-photometer and a fast chemiluminescence instrument [*Zahn et al*., 2012]. Water vapor was measured by a photo-acoustic laser spectrometer and a commercial frost point hygrometer. The measurement of NO is based on the chemiluminescence of excited $NO_2$ molecules formed by reaction of NO with $O_3$ [*Ziereis et al*., 2000; *Stratmann*, 2013]. NO was measured only during daylight.

Figure 1 shows the seasonal variation of acetone, $O_3$, $H_2O$ vapor, and NO relative to the tropopause (TP) at mid-latitudes (35°N–60°N). The distance relative to the TP, $\Delta Z_{TP}(O_3)$, was derived from measured ozone and the well-documented gradient of $O_3$ in the LMS from $O_3$ sondes as described in *Sprung and Zahn* [2010]. $\Delta Z_{TP}(O_3)$ is an in situ measured and mixing-based altitude relative to the thermal TP and is far more accurate than the often used model-based tropopause height retrieved by, e.g., the ECMWF model. All four species (acetone, $O_3$, $H_2O$, NO) show strong vertical gradients in the UT/LMS and considerable seasonal variations. The most prominent features are the well-known descent of ozone-rich stratospheric air in spring within the downward branch of the Brewer-Dobson circulation and the considerable buildup of acetone and water vapor in the summertime UT and its propagation into the LMS. The CARIBIC acetone data set was recently contrasted to results from the LMDz-INCA global chemistry climate model in respect to spatial distribution, temporal variability, and representativeness [*Elias et al*., 2011]. The summer maximum of acetone in the UT can qualitatively be explained by the (i) then peaking emission of precursor species and chemical turnover rates which together lead to maximum photochemical production of acetone, and (ii) by the enhanced lofting of polluted (acetone- and $H_2O$-rich) near-surface air due to convection.

Mixing ratios of NO at the TP are higher between spring and autumn (~180 pptv) compared to winter (~100 pptv) because of (i) stronger photolysis of NO precursors (e.g., $N_2O$ and $HNO_3$), (ii) stronger convective transport of polluted air into the UT, (iii) more frequent lightning events in the northern hemisphere (NH), and (iv) the seasonal cycle of $NO_y$ ($NO_x + HNO_3 + PAN + HONO + N_2O_5 + NO_3 + \ldots$) with enhanced levels in summer. The $NO_x$ winter minimum is not only due to the reduced solar actinic flux but is also associated with the heterogeneous conversion of reactive nitrogen to $HNO_3$ [*Gao et al*., 1997; *Brunner et al*., 2001]. NO above 1000 pptv (~0.6% of the data), mainly caused by fresh contrails and lightning, was not taken into account.

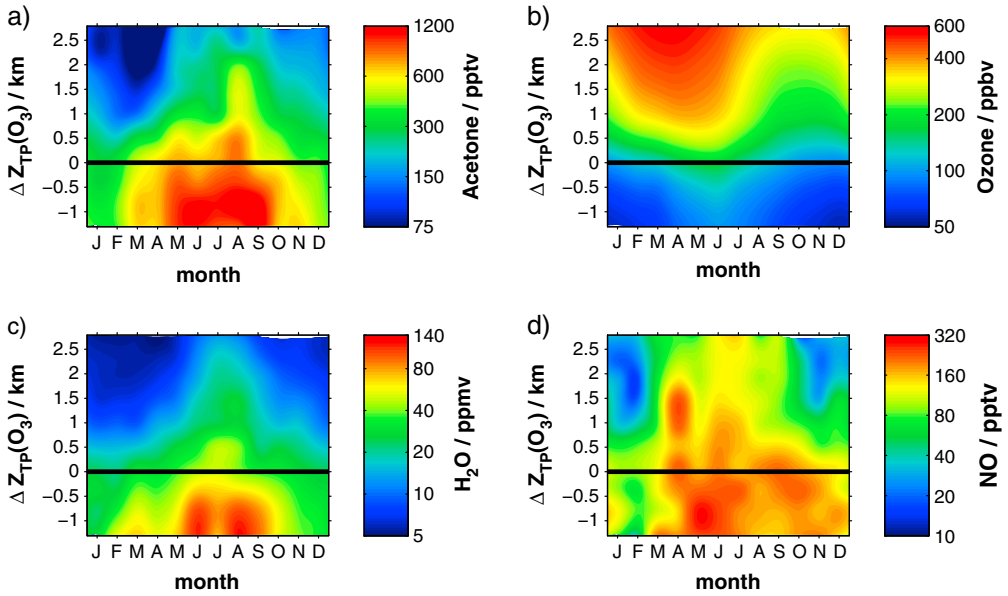


**Figure 1.** Seasonal variation of (a) acetone, (b) ozone, (c) $H_2O$, and (d) NO relative to the thermal TP ($\Delta Z_{TP}(O_3) = 0$, black line) for mid-latitudes (35°N–60°N). The data were collected with CARIBIC between May 2005 and January 2014.

## 3. EMAC Model

Not measured but necessary parameters to infer $HO_x$ production rates were taken from the Chemistry Climate Model EMAC [*Jöckel et al.*, 2006]. This included (a) photolysis rates of acetone, formaldehyde, methyl hydroperoxide, peracetic acid ($CH_3C(O)OOH$), $NO_2$, and $O_3$, (b) the OH and $HO_2$ field, and (c) the temperature field.

EMAC is a combination of the general circulation model ECHAM5 [*Roeckner et al.*, 2006] with a selectable set of submodels such as the chemistry module MECCA1 [*Sander et al.*, 2005] combined through the Modular Earth Submodel System MESSy [*Jöckel et al.*, 2005]. For this study, we performed an EMAC (Version 1.10) simulation from 2008 to 2013 with the horizontal resolution T42 (2.8° × 2.8°) at 39 layers, covering the atmosphere from the surface up to ~80 km (0.01 hPa) and showing a vertical resolution of ~1.3 km at the TP. We applied the identical submodels as described by *Kirner et al.* [2011] and nudged the prognostic variables temperature, vorticity, divergence, and the surface pressure below 1 hPa towards ERA-Interim reanalysis [*Dee et al.*, 2011] to simulate realistic synoptic conditions.

The simulation included a comprehensive atmospheric chemistry setup with reaction rate coefficients following the latest JPL recommendations [*Sander et al.*, 2011]. For this study, photolysis rates $J_i^{\ddagger}$, averaged monthly and zonally between 35°N and 60°N were used. As mean daylight (symbolized by °) photolysis rates $J_i^{\circ}$, we applied as a first approximation

$$J_i^{\circ} = J_i^{\ddagger} \cdot f_s = J_i^{\ddagger} \cdot \frac{24}{(\text{hours of sunlight})_i} \quad (1)$$

where $f_s$ accounts for the number of hours of sunlight in the respective month ranging from ~3.0 in December to ~1.5 in June and July. As $HO_x$ production from acetone (photo)oxidation takes place mainly during daylight, all other parameters (i.e., OH and $HO_2$ from EMAC) were also taken as daylight averaged monthly and zonally means.

The EMAC fields and CARIBIC data were interpolated and binned to the same grid with a vertical resolution of 0.45 km. Diurnally averaged OH and $HO_2$ distributions around the TP from EMAC (not shown) exhibit a strong seasonal variation with the highest concentrations in summer ($[OH] \sim 1.1 \cdot 10^6\,cm^{-3}$, $[HO_2] \sim 2.5 \cdot 10^7\,cm^{-3}$) and significantly smaller concentration in winter ($[OH] \sim 2 \cdot 10^5\,cm^{-3}$, $[HO_2] \sim 1 \cdot 10^7\,cm^{-3}$), in good agreement with *Spivakovsky et al.* [2000]. The corresponding daylight averaged values are higher by a factor of ~1.5 (June) to ~2.5 (December).

## 4. Calculation of $HO_x$ Production Rates $PHO_x(O^1D)$ and $PHO_x(Ac)$

This section outlines the calculation of the $HO_x$ production rates from (a) $O_3$ photolysis and subsequent reaction of $O^1D$ with $H_2O$ denoted by $PHO_x(O^1D)$ and from (b) photolysis of acetone and its reaction with OH denoted by $PHO_x(Ac)$. The most important input parameters—the distributions of the precursor gases $O_3$, $H_2O$, and acetone were taken from CARIBIC (Figures 1a–1c), in the following symbolized by an asterisk. Also, NO, necessary for the calculation of $PHO_x(Ac)$ (see section 4.2), was taken from CARIBIC (Figure 1d).

As $NO_2$ is measured by CARIBIC only during night, daylight $NO_2$ was calculated from the photostationary-state equation [*Westberg et al.*, 1971]

$$[NO_2] = \frac{k_{NO_2} \cdot [NO]^* \cdot [O_3]^*}{J^\circ_{NO_2}} \tag{2}$$

where $k_{NO_2}$ is the rate constant for the $NO + O_3 \rightarrow NO_2 + O_2$ reaction and $J^\circ_{NO_2}$ is the mean daylight photolysis rate of $NO_2$.

### 4.1. $HO_x$ Production Rate From Ozone Photolysis

OH formation *via* photolysis of $O_3$ and subsequent reaction of $O^1D$ with $H_2O$ is given by reaction (3) – (5) [e.g. *Levy*, 1971; *Logan et al.*, 1981; *Monks*, 2005]

$$O_3 + h\nu(\lambda < 320\ nm) \rightarrow O^1D + O_2{}^1\Delta_g \quad J_{O^1D} \tag{3}$$

$$O^1D + H_2O \rightarrow 2OH \quad k_1 \tag{4}$$

$$O^1D + M \rightarrow O^3P + M \quad k_2, k_3 \tag{5}$$

$J(O^1D)$ is the photolysis rate of $O_3$ and $k_1$ the rate constant for reaction (4) taken from *Sander et al.* [2011]. Reaction (5) is the electronic quenching of $O^1D$ due to collisions with $N_2$ ($k_2$) or $O_2$ ($k_3$) [*Sander et al.*, 2011]. The mean daylight $HO_x$ production rate $PHO_x(O^1D)$ then is given by

$$PHO_x(O^1D) = 2 \cdot J(O^1D)^\circ \cdot [O_3]^* \cdot \frac{k_1[H_2O]^*}{k_1[H_2O]^* + k_2[N_2] + k_3[O_2]} \tag{6}$$

$J(O^1D)^\circ$ maximizes with $\sim 2.5 \cdot 10^{-5}\ s^{-1}$ in summer, while the lowest values of $\sim 5 \cdot 10^{-6}\ s^{-1}$ are found in winter (not shown). The seasonal variation of $PHO_x(O^1D)$ relative to the extra-tropical TP (Figure 2a) also maximizes in summer ~1 km below the TP with $\sim 2.7 \cdot 10^4\ cm^{-3}\ s^{-1}$ because of maximizing water VMRs of ~120 ppmv and the then peaking $O_3$ photolysis rate. Conversely, $HO_x$ production rates at the TP bottom out in winter with $\sim 1 \cdot 10^3\ cm^{-3}\ s^{-1}$. The decrease of $PHO_x(O^1D)$ with altitude is strongly correlated with the decrease of water. The summer maximum of $PHO_x(O^1D)$ of $\sim 2.7 \cdot 10^4\ cm^{-3}\ s^{-1}$ is in excellent agreement with $PHO_x(O^1D)$ values given by *Colomb et al.* [2006] for background air in the UT (~10 km altitude) over Europe in July of $3 \cdot 10^{-3}\ ppt\ s^{-1}$ ($\sim 2.5 \cdot 10^4\ cm^{-3}\ s^{-1}$).

### 4.2. $HO_x$ Production Rate From Acetone Photolysis and Reaction With OH

To calculate $HO_x$ production rates from acetone photo(oxidation), we followed the analytical approach by *Folkins and Chatfield* [2000]. As the chemical sinks for acetone are (i) photolysis and (ii) oxidation by OH, the $HO_x$ production rate $PHO_x(Ac)$ is

$$PHO_x(Ac) = HY_{h\nu} \cdot J(Ac)^\circ \cdot [Ac]^* + HY_{OH} \cdot k_{OH} \cdot [OH] \cdot [Ac]^* \tag{7}$$

with $k_{OH}$ the rate constant for the reaction of acetone with OH [*Sander et al.*, 2011], acetone [Ac]* from CARIBIC (Figure 1a) and with $HY_{h\nu}$ and $HY_{OH}$ the net $HO_x$ yields per photolysed or oxidized acetone molecule, respectively. For the photolysis rate $J(Ac)^\circ$, we used the latest JPL recommended values based on QYs by *Blitz et al.* [2004] and *Sander et al.* [2011] as daylight averaged monthly and zonally means.

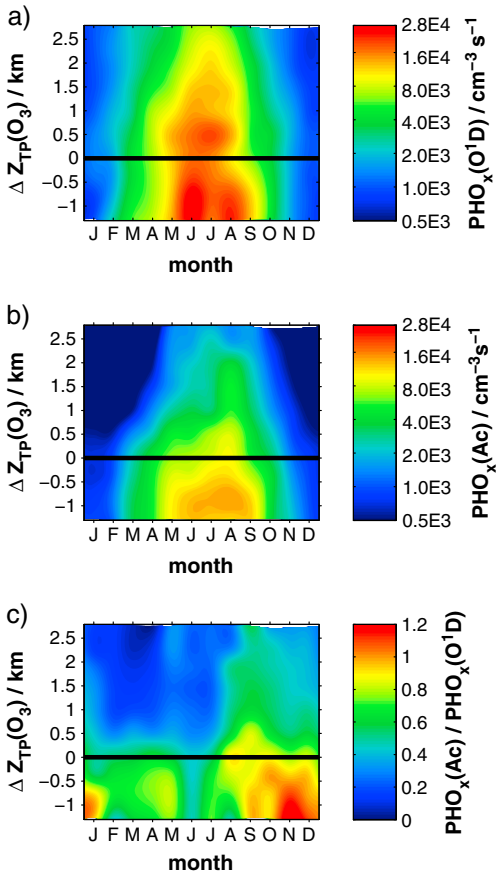


**Figure 2.** (a) Seasonal variation of the daylight mean $HO_x$ production rate $PHO_x(O^1D)$ from ozone photolysis and subsequent reaction of $O^1D$ with water vapor relative to the thermal TP (35°N–60°N). (b) Daylight mean seasonal variation of $PHO_x(Ac)$ calculated by using acetone data from CARIBIC. (c) Ratio $PHO_x(Ac)/PHO_x(O^1D)$.

In accordance with *Folkins and Chatfield* [2000], by introducing a combined, average yield $HY_{avg}$, which is the net number of formed $HO_x$ molecules per each photolysed and oxidized acetone molecule, equation (7) can be expressed as

$$PHO_x(Ac) = HY_{avg} \cdot [Ac]^* \cdot \left(J(Ac)^\circ + k_{OH} \cdot [OH]\right) \quad (8)$$

The yields $HY_{avg}$, $HY_{hv}$, and $HY_{OH}$ are determined by several reactions being part of the (photo)oxidation mechanism of acetone, i.e., reactions of acetone and its oxidation products with $NO_x$, $HO_x$, and several photolysis channels [*Folkins and Chatfield*, 2000]. $HY_{avg}$ depends on NO (taken from CARIBIC), $NO_2$ (from equation (2)), OH, and $HO_2$ (from EMAC) and on the reaction rate constants and photolysis rates of the particular reactions.

### 4.3. Results

As shown in Figure 2b, $PHO_x(Ac)$ shows a pronounced maximum up to ~14,000 $cm^{-3}\,s^{-1}$ in summer ~1 km below the TP that can be traced back to (i) high acetone VMRs (Figure 1), (ii) a high photolysis rate, and (iii) a higher yield $HY_{avg}$ compared to winter (Figure 3). The average $HO_x$ production rate during summer (JJA) amounts to ~8500 $cm^{-3}\,s^{-1}$ at the TP. *Colomb et al.* [2006] estimated $HO_x$ production rates from photolysis of acetone of $0.7 \cdot 10^{-3}$ ppt $s^{-1}$ (~5900 $cm^{-3}\,s^{-1}$) for background air in the UT over Europe in July which is in reasonable agreement with our findings.

Figure 2c shows the ratio $R_{(Ac/O1D)} = PHO_x(Ac)/PHO_x(O^1D)$ that amounts at the TP to ~0.61 on average in summer and to ~0.83 in autumn with values up to ~0.95 in September/October and ~1.2 in November. At higher altitudes, the impact of acetone becomes smaller because of the quickly decreasing acetone VMR, but it is still a noticeable $HO_x$ source with $R_{(Ac/O1D)}$ ranging from ~0.16 (MAM) to ~0.44 (SON) 2.5 km above the TP.

As shown by *Folkins and Chatfield* [2000], $HY_{avg}$ increases rapidly from 0.5 at $NO_x = 5$ pptv to 2.6 at $NO_x = 100$ pptv but increases only slightly above these levels to 2.7 at $NO_x = 1000$ pptv.

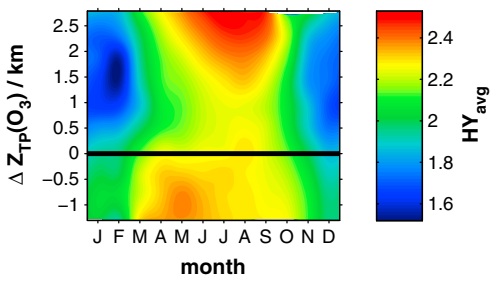


**Figure 3.** Average net $HO_x$ yield (35°N–60°N) for acetone photolysis and reaction with OH based on the and $HO_x$ fields from EMAC and on NO from CARIBIC.

Figure 3 shows the seasonal variation of $HY_{avg}$ based on the $HO_x$ fields from EMAC and on the measured NO (and calculated $NO_2$) from CARIBIC. $HY_{avg}$ maximizes in spring, the lowest values are found in winter above the TP. Photolysis of acetone and oxidation by OH both lead to net production of $HO_x$. The contribution of the acetone + OH reaction to $PHO_x(Ac)$ amounts to ~25% at most at the TP in winter. Ratios of $R_{(Ac/O1D)}$ and $R^{hv}_{(Ac/O1D)}$ (neglecting OH reaction) together with values of $HY_{avg}$, $HY_{hv}$, and $HY_{OH}$ are summarized in Table 1. As shown by *Winkler et al.* [2002], the interaction of acetone with cirrus ice particles is too weak to result in a

**Table 1.** Ratios $R_{(Ac/O1D)}$, $R^{h\nu}_{(Ac/O1D)}$ (Photolysis only), Average $HO_x$ Yield, $HY_{avg}$ and $HY_{h\nu}$ From Acetone Photolysis, and $HY_{OH}$ From Oxidation With OH for Winter (DJF), Spring (MAM), Summer (JJA), and Autumn (SON) at the TP ($\Delta Z_{TP}(O_3) = 0$ km) and 2.5 km Above the TP

| $\Delta Z_{TP}(O_3)$ | | $R_{(Ac/O1D)}$ | $R^{h\nu}_{(Ac/O1D)}$ | $HY_{avg}$ | $HY_{h\nu}$ | $HY_{OH}$ |
|---|---|---|---|---|---|---|
| 0 km | DJF | 0.61 | 0.48 | 1.93 | 2.84 | 0.90 |
| | MAM | 0.58 | 0.48 | 2.20 | 2.93 | 0.98 |
| | JJA | 0.61 | 0.51 | 2.27 | 2.95 | 1.00 |
| | SON | 0.83 | 0.67 | 2.12 | 2.95 | 1.00 |
| 2.5 km | DJF | 0.22 | 0.19 | 1.81 | 2.56 | 0.66 |
| | MAM | 0.16 | 0.14 | 2.19 | 2.76 | 0.82 |
| | JJA | 0.27 | 0.24 | 2.45 | 2.92 | 0.96 |
| | SON | 0.44 | 0.38 | 2.18 | 2.77 | 0.87 |

significant partition to the ice phase so that the role of acetone as an $HO_x$ precursor is not perturbed by the presence of cirrus clouds.

Figure 4 shows $R_{(Ac/O1D)}$ as a function of $H_2O$ from winter to autumn. Using photolysis rates based on the latest QYs acetone (photo)oxidation can still be considered a significant ($R_{(Ac/O1D)} > 0.5$) $HO_x$ source at water VMRs below ~100 ppmv (in summer/autumn) and reaches values up to ~1.2 between 30 and 50 ppmv in autumn. Our analysis is in good agreement with *Jaeglé et al.* [2001] using *Gierczak* QYs-based photolysis rates, i.e., acetone degradation becomes a dominant ($R_{(Ac/O1D)} > 1$) $HO_x$ source below ~120 ppmv water vapor (not shown).

## 5. Sensitivity Study

In a sensitivity study, we verified the uncertainty of our results by varying different input parameters.

### 5.1. NO From CARIBIC

NO from CARIBIC ranges from 111 ± 100 pptv (DJF) to 188 ± 106 pptv (SON) at the TP and between 30 ± 42 (DJF) and 127 ± 75 pptv (JJA) 2.5 km above the TP. In the troposphere, NO is highly variable, and mixing ratios differ quite strongly dependent on the sampled region, e.g., 257 ± 252 pptv in spring over North America or 276 ± 414 pptv in autumn over North Asia [*Stratmann*, 2013]. The lowest tropospheric mixing ratios during summer are observed over North America (99 ± 104 pptv) and during winter over the North Atlantic (54 ± 49 pptv) [*Stratmann*, 2013].

A comparison of CARIBIC data with data observed during the NOXAR (Nitrogen OXides along Air Routes) project shows good agreement concerning the seasonal NO cycle over Europe/Asia and over the North Atlantic with maxima during summer. However, mixing ratios deviate partially strongly, which was to large part traced back to differences in flight routes [*Brunner et al.*, 2001; *Stratmann*, 2013].

When considering longitudinal-averaged mixing ratios, deviations between CARIBIC and NOXAR largely cancel out. For instance typical upper-tropospheric $NO_x$ mixing ratios during NOXAR were 100 ± 50 pptv (winter) and 150 ± 100 pptv (summer) with up to ~230 pptv at the TP in summer, while the highest levels were typically located 2–3 km below the TP [*Grewe et al.*, 2001].

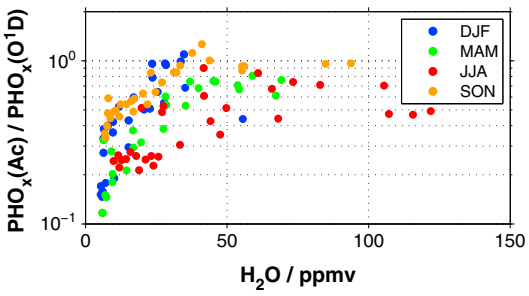


**Figure 4.** Ratio $PHO_{x(Ac)}/PHO_x(O^1D)$ versus water vapor from CARIBIC for winter (DJF), spring (MAM), summer (JJA), and autumn (SON).

As a test, we scaled the NO field from CARIBIC (and the derived $NO_2$ field) by a factor of 0.5 (scenario **1**) and 2 (scenario **2**), respectively, while leaving the EMAC $HO_x$ fields unchanged. The results (see Table 2) stay basically the same: $R_{(Ac/O1D)}$ changes at most in winter 2.5 km above the TP by ~−8% (scenario **1**) and by ~4% (scenario **2**). This is because $NO_x$ in the NH UT is high enough so that $HY_{avg}$ changes only slightly with varying $NO_x$. Therefore, $NO_x$ is not a critical parameter.

**Table 2.** Ratio $R_{(Ac/O1D)}$ and Changes of $R_{(Ac/O1D)}$ (in %) Upon Scaling the Input Parameters by the Factors Given in Parentheses[a]

| $\Delta Z_{TP}(O_3)$ | | $R_{(Ac/O1D)}$ | 1 NO (0.5) | 2 NO (2) | 3 OH, $HO_2$ (1.3,1.5) | 4 $J(O^1D)$ (0.7,1.3) | 5 $J$(Ac) (0.8,1.2) |
|---|---|---|---|---|---|---|---|
| 0 km | DJF | 0.61 | −4.5 | 2.3 | 2.2 | 43/−23 | −16/16 |
| | MAM | 0.58 | −4.1 | 2.1 | 0.6 | 43/−23 | −17/17 |
| | JJA | 0.61 | −4.1 | 2.1 | −0.3 | 43/−23 | −17,17 |
| | SON | 0.83 | −3.4 | 1.7 | 1.5 | 43/−23 | −16/16 |
| 2.5 km | DJF | 0.22 | −8.3 | 4.4 | −2.5 | 43/−23 | −17/17 |
| | MAM | 0.16 | −3.8 | 1.9 | −0.8 | 43/−23 | −18/18 |
| | JJA | 0.27 | −3.5 | 1.8 | −1.0 | 43/−23 | −18/18 |
| | SON | 0.44 | −7.7 | 4.0 | −3.0 | 43/−23 | −18/18 |

[a]Scenarios 1–5 (see text).

### 5.2. EMAC $HO_x$ Field

Recently, *Regelin et al*. [2013] have shown that calculated $HO_x$ levels from EMAC in the upper-troposphere (7–10 km) over Europe significantly underestimate observed levels by ~24% (OH) and ~41% ($HO_2$). Upon scaling the OH/$HO_2$ field by factors of 1.3/1.5 (scenario **3**), while leaving all other parameters unchanged (Table 2), $R_{(Ac/O1D)}$ decreases at most by ~ −3% 2.5 km above the TP in autumn.

### 5.3. Photolysis Rates

For the photolysis cross sections and quantum yields of ozone, a combined uncertainty of 1.3 is given by *Sander et al*. [2011] which will be used here as the uncertainty of the $O_3$ photolysis rate. Scaling $J(O^1D)$ by factors of 0.7 and 1.3, respectively, leads to changes of ~43% and ~ −23% of $R_{(Ac/O1D)}$ at the TP (scenario **4**). For the photolysis rate of acetone, we assume an uncertainty factor of 1.2, based on the overall error of 10–15% for the parameterization of the QYs given by *Blitz et al*. [2004] which directly converts into a $R_{(Ac/O1D)}$ change of ~ ±17% at the TP (scenario **5**).

All other used photolysis rates affect the result only indirectly by influencing the yield $HY_{avg}$. For instance, scaling $J(NO_2)$ by its combined uncertainty of 1.2 leads only to small changes of $R_{(Ac/O1D)}$ by 1–3%. The impact on $R_{(Ac/O1D)}$ upon scaling $J(CH_2O)$ by its uncertainty factor of 1.4 [*Sander et al*., 2011] is even less pronounced with small increases up to ~2%.

In summary, we estimate the total uncertainty of the acetone $HO_x$ production rate by using Gaussian error propagation to ~35% (30% estimated uncertainty being the sum of instrumental uncertainty and the limited representativeness of the data and 20% uncertainty of the acetone photolysis rates).

## 6. Summary

The $HO_x$ source from acetone degradation $PHO_x$(Ac) due to photolysis and reaction with OH was quantified and compared with the $HO_x$ source from ozone photolysis $PHO_x(O^1D)$ in the mid-latitude UT/LMS. Representative distributions of acetone, ozone, water vapor, and NO collected onboard the CARIBIC passenger aircraft between 2005 and 2014 at 9–12 km at mid-latitudes were considered. Not detected parameters like photolysis rates and $HO_x$ distributions were taken from the global chemistry model EMAC.

Year-around, acetone was found to be an important precursor of $HO_x$ around the mid-latitude TP. Typical summer values of $PHO_x$(Ac) amount to ~ 8500 $cm^{-3} \cdot s^{-1}$ with a maximum of 14,000 $cm^{-3} \cdot s^{-1}$ ~ 1 km below the TP which is on average ~60% of the $HO_x$ production rate from ozone photolysis. The strongest impact by acetone is observed in autumn when $PHO_x$(Ac) is up to ~95% of $PHO_x(O^1D)$, i.e., when the UT is already quite dry with $H_2O \approx 30 - 50$ ppmv but still rich in acetone with on average ~500 pptv. Above the TP, the impact from acetone decreases due to the quickly decreasing acetone levels and reaches at 2.5 km above the TP ~ 44% in autumn.

In a sensitivity study, the uncertainty of our findings was quantified, and the parameters that impact them most were identified. It was demonstrated that besides the photolysis rates of acetone the acetone

distribution is the most sensitive input parameter. This is a crucial point, as in the past no representative distributions of acetone in the UT/LMS have been available. We studied the influence of (i) the CARIBIC NO distribution which affects the yield of formed $HO_x$ species during the degradation of acetone, (ii) of the OH and $HO_2$ fields from EMAC, and (iii) of several photolysis rates. Scaling the CARIBIC NO field by factors of 0.5 and 2, which results in unrealistically low (high) NO levels, changes $R_{(Ac/O1D)}$ by −5–2% at the TP. The dependence on the $OH/HO_2$ is comparable with $R_{(Ac/O1D)}$ changing by ~ 2% in winter upon scaling the OH and $HO_2$ field by a factor of 1.3 and 1.5. Altogether, the sensitivity study in section 5 indicates that the uncertainty of the inferred acetone-derived $HO_x$ production rates in the UT/LMS is ~35%.

**Acknowledgments**

We are deeply indebted to Andreas Waibel, Lufthansa for successfully guiding the scientific project CARIBIC. Likewise, we thank the operational flight planners, Mrs. Sieglinde Bacher and Mr. Peter Hartleib. CARIBIC obtains as part of IAGOS (www.iagos.org) funding from the Germany Ministry of Science and Education. We also acknowledge financial help from Frankfurt Airport, Fraport AG, and the Max Planck Society. Further, the authors would like to thank John Crowley (MPIC, Mainz) for discussions.

The Editor thanks two anonymous reviewers for their assistance in evaluating this paper.

## References

Arnold, S. R., M. P. Chipperfield, M. A. Blitz, D. E. Heard, and M. J. Pilling (2004), Photodissociation of acetone: Atmospheric implications of temperature-dependent quantum yields, *Geophys. Res. Lett.*, *31*, L07110, doi:10.1029/2003GL019099.

Arnold, F., V. Bürger, B. Droste-Fanke, F. Grimm, A. Krieger, J. Schneider, and T. Stilp (1997), Acetone in the upper troposphere and lower stratosphere: Impact on trace gases and aerosols, *Geophys. Res. Lett.*, *24*(23), 3017–3020, doi:10.1029/97GL02974.

Arnold, S. R., M. P. Chipperfield, and M. A. Blitz (2005), A three-dimensional model study of the effect of new temperature-dependent quantum yields for acetone photolysis, *J. Geophys. Res.*, *110*, 22305, doi:10.1029/2005JD005998.

Atkinson, R., D. L. Baulch, R. A. Cox, J. N. Crowley, R. F. Hampson, R. G. Hynes, M. E. Jenkin, M. J. Rossi, and J. Troe (2006), Evaluated kinetic and photochemical data for atmospheric chemistry: Volume II – gas phase reactions of organic species, *Atmos. Chem. Phys.*, *6*(11), 3625–4055, doi:10.5194/acp-6-3625-2006.

Blitz, M. A., D. E. Heard, M. J. Pilling, S. R. Arnold, and M. P. Chipperfield (2004), Pressure and temperature-dependent quantum yields for the photodissociation of acetone between 279 and 327.5 nm, *Geophys. Res. Lett.*, *31*, L06111, doi:10.1029/2003GL018793.

Brenninkmeijer, C. A. M., et al. (2007), Civil Aircraft for the regular investigation of the atmosphere based on an instrumented container: The new CARIBIC system, *Atmos. Chem. Phys.*, *7*(18), 4953–4976, doi:10.5194/acp-7-4953-2007.

Brunner, D., J. Staehelin, D. Jeker, H. Wernli, and U. Schumann (2001), Nitrogen oxides and ozone in the tropopause region of the northern hemisphere: Measurements from commercial aircraft in 1995/1996 and 1997, *J. Geophys. Res.*, *106*(D21), 27,673–27,699, doi:10.1029/2001JD900239.

Colomb, A., et al. (2006), Airborne measurements of trace organic species in the upper troposphere over Europe: The impact of deep convection, *Environ. Chem.*, *3*(4), 244–259, doi:10.1071/EN06020.

Dee, D. P., et al. (2011), The ERA-Interim reanalysis: Configuration and performance of the data assimilation system, *Q. J. R. Meteorol. Soc.*, *137*(656), 553–597, doi:10.1002/qj.828.

Elias, T., S. Szopa, A. Zahn, T. Schuck, C. Brenninkmeijer, D. Sprung, and F. Slemr (2011), Acetone variability in the upper troposphere: Analysis of CARIBIC observations and LMDz-INCA chemistry-climate model simulations, *Atmos. Chem. Phys.*, *11*(15), 8053–8074, doi:10.5194/acp-11-8053-2011.

Folkins, I., and R. Chatfield (2000), Impact of acetone on ozone production and OH in the upper troposphere at high $NO_x$, *J. Geophys. Res.*, *105*(D9), 11,585–11,599, doi:10.1029/2000JD900067.

Gao, R. S., et al. (1997), Partitioning of the reactive nitrogen reservoir in the lower stratosphere of the southern hemisphere: Observations and modeling, *J. Geophys. Res.*, *102*(D3), 3935–3949, doi:10.1029/96JD01967.

Gierczak, T., J. B. Burkholder, S. Bauerle, and A. R. Ravishankara (1998), Photochemistry of acetone under tropospheric conditions, *Chem. Phys.*, *231*(2–3), 229–244, doi:10.1016/S0301-0104(98)00006-8.

Grewe, V., D. Brunner, M. Dameris, J. L. Grenfell, R. Hein, D. Shindell, and J. Staehelin (2001), Origin and variability of upper tropospheric nitrogen oxides and ozone at northern mid-latitudes, *Atmos. Environ.*, *35*(20), 3421–3433, doi:10.1016/S1352-2310(01)00134-0.

Jaeglé, L., D. J. Jacob, W. H. Brune, and P. O. Wennberg (2001), Chemistry of $HO_x$ radicals in the upper troposphere, *Atmos. Environ.*, *35*(3), 469–489, doi:10.1016/S1352-2310(00)00376-9.

Jaeglé, L., et al. (1997), Observed OH and $HO_2$ in the upper troposphere suggest a major source from convective injection of peroxides, *Geophys. Res. Lett.*, *24*(24), 3181–3184, doi:10.1029/97GL03004.

Jaeglé, L., et al. (2000), Photochemistry of $HO_x$ in the upper troposphere at northern midlatitudes, *J. Geophys. Res.*, *105*(D3), 3877–3892, doi:10.1029/1999JD901016.

Jöckel, P., R. Sander, A. Kerkweg, H. Tost, and J. Lelieveld (2005), Technical Note: The Modular Earth Submodel System (MESSy) - a new approach towards Earth System Modeling, *Atmos. Chem. Phys.*, *5*(2), 433–444, doi:10.5194/acp-5-433-2005.

Jöckel, P., et al. (2006), The atmospheric chemistry general circulation model ECHAM5/MESSy1: Consistent simulation of ozone from the surface to the mesosphere, *Atmos. Chem. Phys. Discuss.*, *6*(4), 6957–7050, doi:10.5194/acpd-6-6957-2006.

Khamaganov, V. G., and J. N. Crowley (2013), Pressure dependent photolysis quantum yields for $CH_3C(O)CH_3$ at 300 and 308 nm and at 298 and 228 K, *Phys. Chem. Chem. Phys.*, *15*(25), 10,500–10,509, doi:10.1039/c3cp50291k.

Kirner, O., R. Ruhnke, J. Buchholz-Dietsch, P. Jöckel, C. Brühl, and B. Steil (2011), Simulation of polar stratospheric clouds in the chemistry-climate-model EMAC via the submodel PSC, *Geosci. Model Dev.*, *4*(1), 169–182, doi:10.5194/gmd-4-169-2011.

Levy, H., II (1971), Normal atmosphere: Large radical and formaldehyde concentrations predicted, *Science*, *173*(3992), 141–143, doi:10.1126/science.173.3992.141.

Logan, J. A., M. J. Prather, S. C. Wofsy, and M. B. McElroy (1981), Tropospheric chemistry: A global perspective, *J. Geophys. Res.*, *86*(C8), 7210–7254, doi:10.1029/JC086iC08p07210.

Monks, P. S. (2005), Gas-phase radical chemistry in the troposphere, *Chem. Soc. Rev.*, *34*(5), 376–395, doi:10.1039/b307982c.

Müller, J.-F., and G. Brasseur (1999), Sources of upper tropospheric $HO_X$: A three-dimensional study, *J. Geophys. Res.*, *104*(D1), 1705–1715, doi:10.1029/1998JD100005.

Nádasdi, R., G. Kovács, I. Szilágyi, A. Demeter, S. Dóbé, T. Bérces, and F. Márta (2007), Exciplex laser photolysis study of acetone with relevance to tropospheric chemistry, *Chem. Phys. Lett.*, *440*(1–3), 31–35, doi:10.1016/j.cplett.2007.04.014.

Prinn, R. G. (2003), The cleansing capacity of the atmosphere, *Annu. Rev. Environ. Resour.*, *28*(1), 29–57, doi:10.1146/annurev.energy.28.011503.163425.

Regelin, E., et al. (2013), $HO_x$ measurements in the summertime upper troposphere over Europe: A comparison of observations to a box model and a 3-D model, *Atmos. Chem. Phys.*, *13*(21), 10,703–10,720, doi:10.5194/acp-13-10703-2013.

Roeckner, E., R. Brokopf, M. Esch, M. Giorgetta, S. Hagemann, L. Kornblueh, E. Manzini, U. Schlese, and U. Schulzweida (2006), Sensitivity of simulated climate to horizontal and vertical resolution in the ECHAM5 atmosphere model, *J. Clim.*, *19*(16), 3771–3791, doi:10.1175/JCLI3824.1.

Sander, R., A. Kerkweg, P. Jöckel, and J. Lelieveld (2005), Technical note: The new comprehensive atmospheric chemistry module MECCA, *Atmos. Chem. Phys.*, *5*(2), 445–450, doi:10.5194/acp-5-445-2005.

Sander, S. P., et al. (2011), Chemical kinetics and photochemical data for use in atmospheric studies, Evaluation Number 17, JPL Publication *10-6*(17), Jet Propulsion Laboratory, Pasadena, Calif. [Available at http://jpldataeval.jpl.nasa.gov.]

Singh, H. B., M. Kanakidou, P. J. Crutzen, and D. J. Jacob (1995), High concentrations and photochemical fate of oxygenated hydrocarbons in the global troposphere, *Nature*, *378*(6552), 50–54, doi:10.1038/378050a0.

Spivakovsky, C. M., et al. (2000), Three-dimensional climatological distribution of tropospheric OH: Update and evaluation, *J. Geophys. Res.*, *105*(D7), 8931–8980, doi:10.1029/1999JD901006.

Sprung, D., and A. Zahn (2010), Acetone in the upper troposphere/lowermost stratosphere measured by the CARIBIC passenger aircraft: Distribution, seasonal cycle, and variability, *J. Geophys. Res.*, *115*, D16301, doi:10.1029/2009JD012099.

Stratmann, G. (2013), Stickoxidmessungen in der Tropopausenregion an Bord eines Linienflugzeugs: Großräumige Verteilung und Einfluss des Luftverkehrs, Technische Univ. München, Munich, Germany.

Warneke, C., J. A. de Gouw, W. C. Kuster, P. D. Goldan, and R. Fall (2003), Validation of atmospheric VOC measurements by proton-transfer-reaction mass spectrometry using a gas-chromatographic preseparation method, *Environ. Sci. Technol.*, *37*(11), 2494–2501, doi:10.1021/es026266i.

Wennberg, P. O., et al. (1998), Hydrogen radicals, nitrogen radicals, and the production of $O_3$ in the upper troposphere, *Science*, *279*(5347), 49–53, doi:10.1126/science.279.5347.49.

Westberg, K., N. Cohen, and K. W. Wilson (1971), Carbon monoxide: Its role in photochemical smog formation, *Science*, *171*(3975), 1013–1015, doi:10.1126/science.171.3975.1013.

Winkler, A. K., N. S. Holmes, and J. N. Crowley (2002), Interaction of methanol, acetone and formaldehyde with ice surfaces between 198 and 223 K, *Phys. Chem. Chem. Phys.*, *4*(21), 5270–5275, doi:10.1039/b206258e.

Wróblewski, T., L. Ziemczonek, A. M. Alhasan, and G. P. Karwasz (2007), Ab initio and density functional theory calculations of proton affinities for volatile organic compounds, *Eur. Phys. J. Spec. Top.*, *144*(1), 191–195, doi:10.1140/epjst/e2007-00126-7.

Zahn, A., J. Weppner, H. Widmann, K. Schlote-Holubek, B. Burger, T. Kühner, and H. Franke (2012), A fast and precise chemiluminescence ozone detector for eddy flux and airborne application, *Atmos. Meas. Tech.*, *5*(2), 363–375, doi:10.5194/amt-5-363-2012.

Ziereis, H., H. Schlager, P. Schulte, P. F. J. van Velthoven, and F. Slemr (2000), Distributions of NO, $NO_x$, and $NO_y$ in the upper troposphere and lower stratosphere between 28° and 61°N during POLINAT 2, *J. Geophys. Res.*, *105*(D3), 3653–3664, doi:10.1029/1999JD900870.